

New UWB Monopole Planer Antenna with Dual Band Notched

Mojtaba Mighani^{1, *} and Mohammad Akbari²

Abstract—A new compact antenna with the capability of covering Ultra Wide Band (UWB) Communication is presented. The size of the antenna is $22 \times 24 \text{ mm}^2$. Moreover, the proposed antenna has been successfully fabricated and measured, showing broadband matched impedance ($\sim 149\%$, 2.1 up to more than 14.3 GHz, $\text{VSWR} \leq 2$). Also the antenna has dual band rejected characteristic on WLAN and WiMAX bands. Frequency and time domain performances of the antenna such as fidelity factor are examined at the end of the paper.

1. INTRODUCTION

Nowadays, due to developing wireless broadband communications systems, plenty of UWB antennas are considered. Microstrip monopole antenna is one of the suitable antennas to use in UWB frequency band because of lower construction expenses, broadband width, compact dimensions, and finally it is possible to integrate with kinds of RF circuits. The patch of this type of reported antennas has different shapes such as rectangular, disc, triangle and oval forms [1–6]. There are many techniques that consist of changes on patch, feed line, and ground structure which is introduced as the most important of all to enhance the bandwidth and access to UWB bandwidth [7, 8]. On the other hand, the frequency range for UWB systems will cause interference with existing narrowband wireless communication systems, for example, the wireless local area network (WLAN) for IEEE 802.11a operating at 5.15–5.35 and 5.725–5.825 GHz, and the Worldwide Interoperability for microwave access (WiMAX) for IEEE 802.16 operating at 3.4–3.69, 5.25–5.85 GHz. Therefore, UWB antennas with band-notched characteristics for filtering the potential interference are desirable. Today, many UWB antennas with various band-notched properties have been developed, and growing research activity is focused on application in multi-input-multi-output (MIMO) systems [9–11]. The use of one circular slot technique on the ground right under the feed line has achieved a bandwidth as much as 149% with complete UWB covering. Consequently, the antenna with compact dimensions and much extended bandwidth is a suitable option for all UWB communication systems. Moreover, the proposed antenna can be used in UWB systems which need no filters to suppress dispensable bands. Both the Ansoft High Frequency Simulation Structure (HFSS) [12] and Computer Simulation Technology (CST) [13] three-dimensional (3-D) electromagnetic EM simulators are used to optimize the presented design. The dual-band notch was successfully implemented, and the simulated results show reasonable agreement with the measured ones. Rest of the paper is organized as following. Section 2 describes the antenna design. Discussions on results are presented in Section 3, followed by conclusive comments and further scope in Section 4.

2. ANTENNA DESIGN

The geometry and photograph of the fabricated antenna are depicted in Figure 1. The optimized values of parameters are listed in Table 1. The antenna is printed on a $22 \times 24 \text{ mm}^2$ FR4 substrate with

Received 30 May 2014, Accepted 19 July 2014, Scheduled 11 August 2014

* Corresponding author: Mojtaba Mighani (mojtaba.mighani@gmail.com).

¹ Faculty of Electrical Engineering, Aeronautical University, Tehran, Iran. ² Department of Electrical and Computer Engineering, Concordia University, Montreal, QC, Canada.

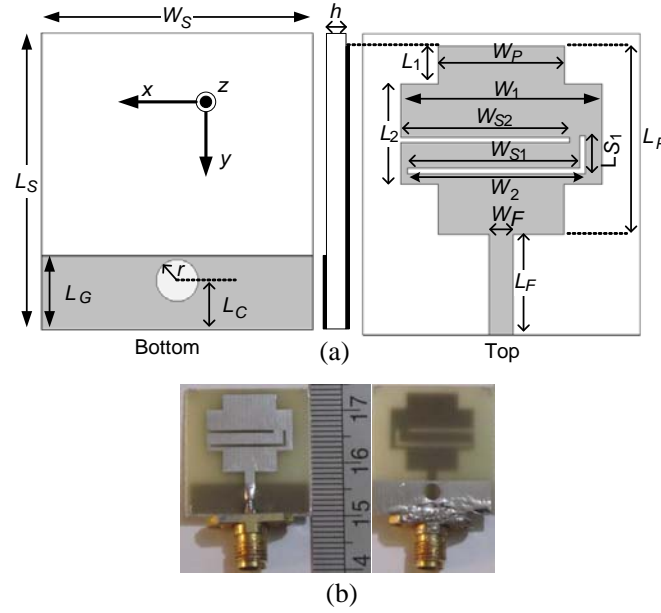


Figure 1. (a) Geometry and (b) photo of the fabricated antenna.

Table 1. Parameter values of the fabricated antenna in mm.

L_1	L_2	L_F	L_P	L_C	L_S
3	8	8	15	4	24
L_{S1}	L_G	W_1	W_2	W_S	W_{S1}
3.1	6	16	14.2	22	13.7
W_{S2}	W_F	W_P	r	h	ϵ_r
12.4	1.9	10	1.7	1	4.4

relative permittivity 4.4 and thickness 1 mm. Radiation element is fed by using a line 50 ohm. To have characteristic impedance 50 ohm, by using AWR2008 software [14], the width of feed line (W_F) is calculated 1.9 mm. The next section is about antenna design process and the effect of various parameters on VSWR.

2.1. Full-Band Design

As shown in Figure 2, adding one rectangular plate to primary radiation element can significantly improve matching impedance at frequencies higher than 9 GHz. According to Figure 2, the best value for W_1 parameter is 16 mm. Continually, the bandwidth from 2.1 GHz to 14.3 GHz will be increased by using the technique in [7]. This technique is to add one circular slot on the ground right under feed line. Regarding to Figure 3, UWB bandwidth will be covered completely by creating and enhancing the radius of circular slot to 1.7 mm.

2.2. Dual Band-Notches Design

Filtering interferences of WiMAX and WLAN bands are one of the designers' main goals. To deal with it, the effect of each slot on the radiation patch is exhibited alone or beside each other in Figure 4. Based on the method introduced in papers as [9, 13], using a slot on antenna radiation patch can obtain resonant frequency and filter desired frequency according to slot length. If the slot is etched on radiation patch completely, the relation between slot length and notched frequency corresponds to (2).

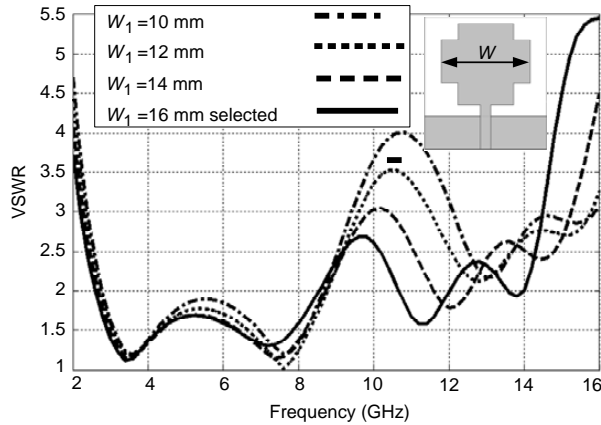


Figure 2. Simulated VSWR of the referenced antenna without slot for different values of W_1 .

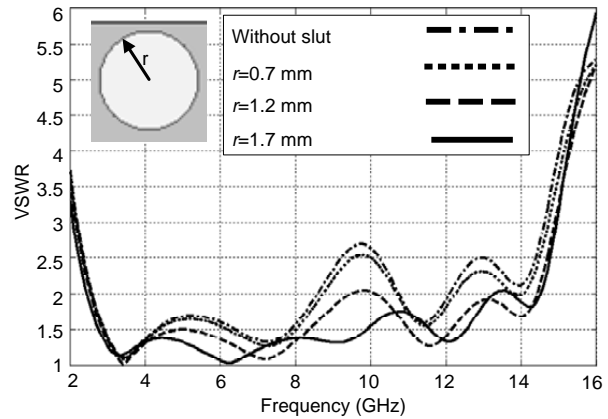


Figure 3. Simulated VSWR of the referenced antenna for different values of r .

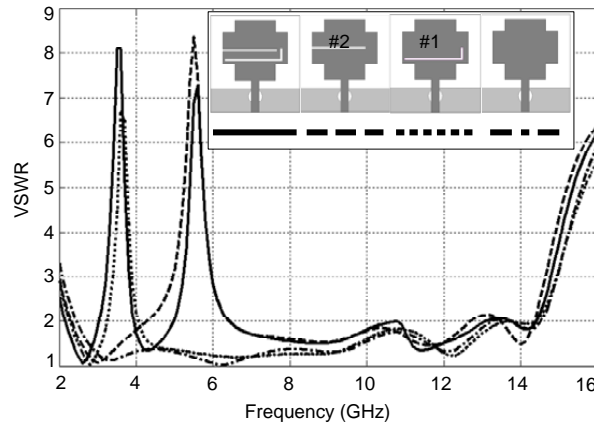


Figure 4. The effect of each patch slots on VSWR.

With regard to the desirable resonant frequency which is 5.5 GHz, length of the slot #1 is calculated 16.6 mm that is matched with $W_2 + L_{S1}$ as defined in Figure 1 and Table 1. Based on the method introduced in paper [9], using a slot which includes the edge of radiation patch can easily obtain considered resonant frequency to filter the interference. Meanwhile, the length of this kind of slots containing the edge of radiation patch corresponds to Equation (3).

$$\epsilon_{re} = \frac{1 + \epsilon_r}{2}, \tag{1}$$

$$L = \frac{\lambda_g}{2} = \frac{300}{2f \text{ (GHz)} \sqrt{\epsilon_{re}}} \tag{2}$$

$$L = \frac{\lambda_g}{4} = \frac{300}{4f \text{ (GHz)} \sqrt{\epsilon_{re}}} \tag{3}$$

Therefore a slot with length of $W_{S2} = 12$ is needed for resonant frequency 3.6 GHz (through 3). To be more clear, it is better to consider current distribution at notched frequencies. Obviously, according to Figure 5(a), the length of slot is $\lambda/4$ while the length of current distribution at frequency 3.6 GHz is $\lambda/2$ because the current begins from point A which is minimal, and then it reaches point B, which is the maximum and is ultimately ended up at point C, which is the minimum too. Moreover, from Figure 5(b) it can be concluded that the length of slot is $\lambda/2$ while the length of current distribution at frequency 3.6 GHz is λ because the current begins from point A and is eventually ended up at point E.

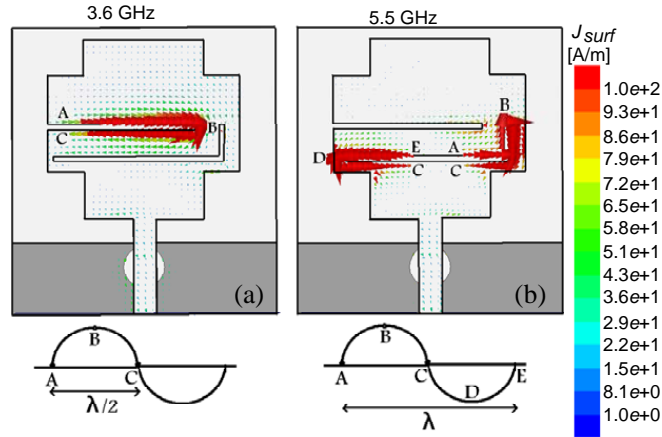


Figure 5. Simulated current distribution on the patch at frequencies, (a) 3.6 GHz, (b) 5.5 GHz.

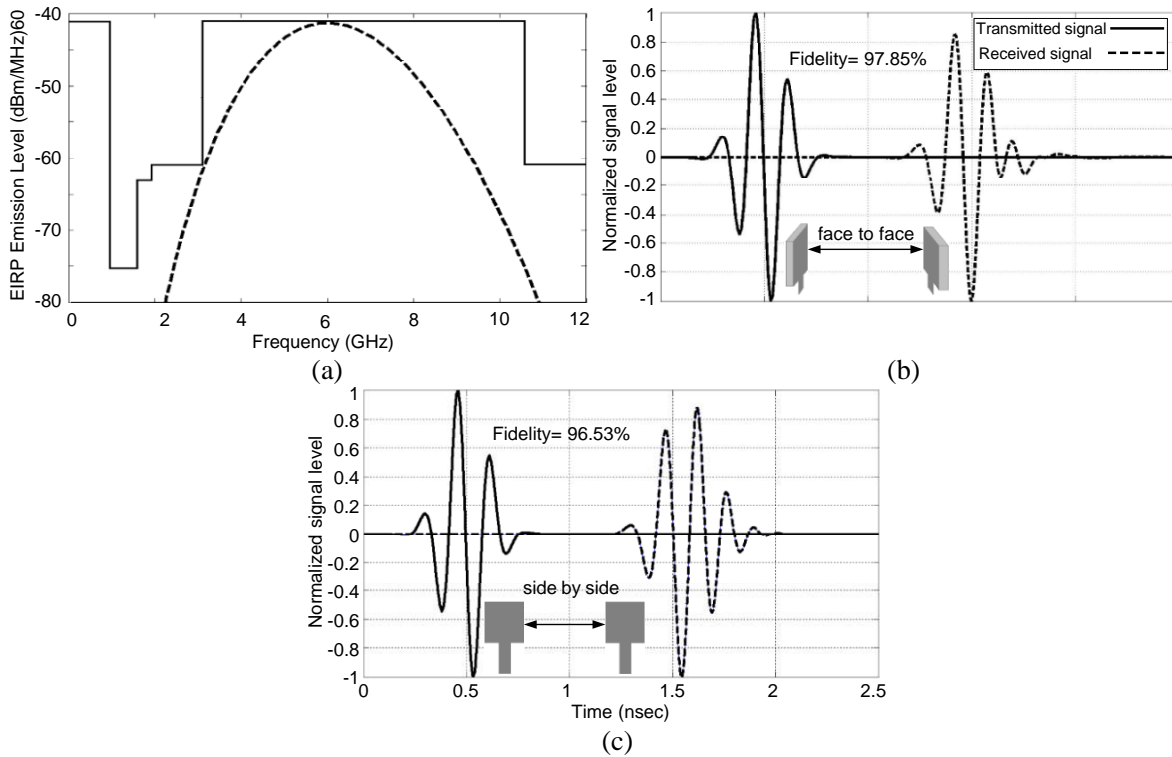


Figure 6. (a) Power spectrum density compared to FCC mask and transmitted and received pulses in time domain for a UWB link with two identical (b) face-to-face and (c) side by side antenna without notches.

3. RESULTS AND DISCUSSIONS

This section includes three parts: time-domain analysis, frequency-domain analysis and measurements.

3.1. Time-Domain Analysis

Computation of the dispersion that occurs when the antenna radiates and receives a pulse signal is very important. The transmit transfer functions of the antennas were used to compute the radiated pulse in different directions when a reference signal was applied at the antenna input. This signal should

present an UWB spectrum covering the antenna bandwidth and particularly the FCC mask from 3.1 to 10.6 GHz. It is shown in Figure 6 that an acceptable approximation to a FCC mask compliant pulse can be obtained with a Gaussian 7th derivative. N th Gaussian pulse is represented in the time domain by (5). In this formula, $H_n(t)$ is the n th Hermit polynomial.

$$G(t) = A \cdot \exp\left(-\frac{t^2}{2\sigma^2}\right) \tag{4}$$

$$G^n(t) = \frac{d^n G}{dt^n} = (-1)^n \frac{1}{(\sqrt{2}\sigma)^2} \cdot H_n\left(\frac{t}{\sqrt{2}\sigma}\right) \cdot G(t) \tag{5}$$

$$H_7(t) = 128t^7 - 1344t^5 + 3360t^3 - 1680t \tag{6}$$

This signal and its spectrum are represented in Figure 6. The pulse bandwidth in frequency domain (power spectrum density) is exactly into the mask defined by FCC. Unfortunately, this subject has never been paid attention in many papers, and designers use Gaussian pulses with under seventh derivative, which can have tangible errors. Luckily, after drawing various Gaussian pulses from the first to eighth derivative, it was obtained that the best pulse for covering FCC mask can be the seventh derivative. Of course with a bit tolerance, the sixth and eighth derivatives are acceptable.

In telecommunications systems, the correlation between the transmitted (TX) and received (RX)

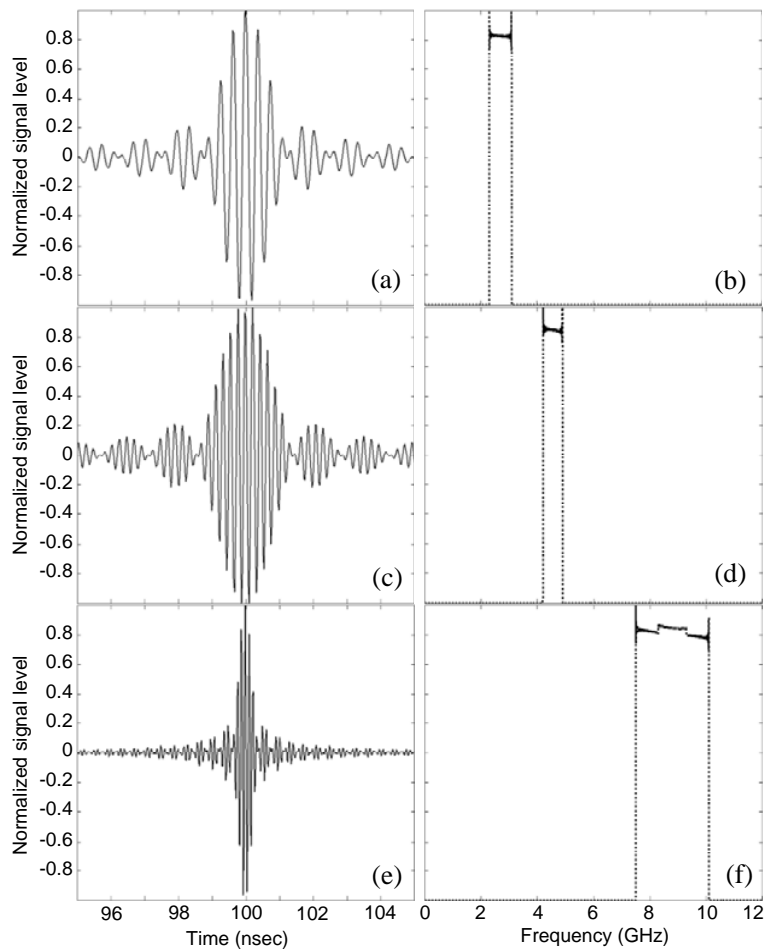


Figure 7. (a), (c) (e) Sync pulses in three different frequencies 2.7, 4.5, 8.5 GHz and (b), (d), (f) their Power Spectrum Density.

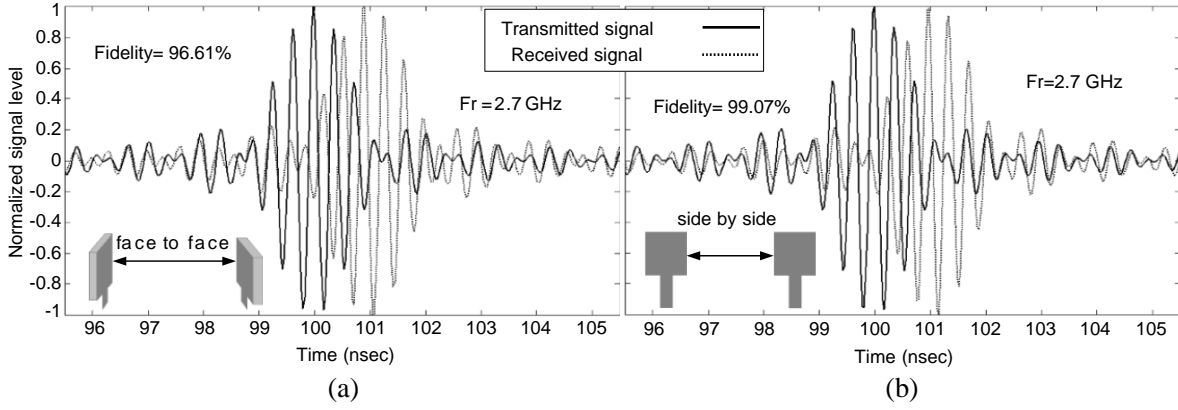


Figure 8. Sync pulses transmitted and received in time domain with two identical (a) face-to-face and (b) side by side the antennas with notches in first frequency band.

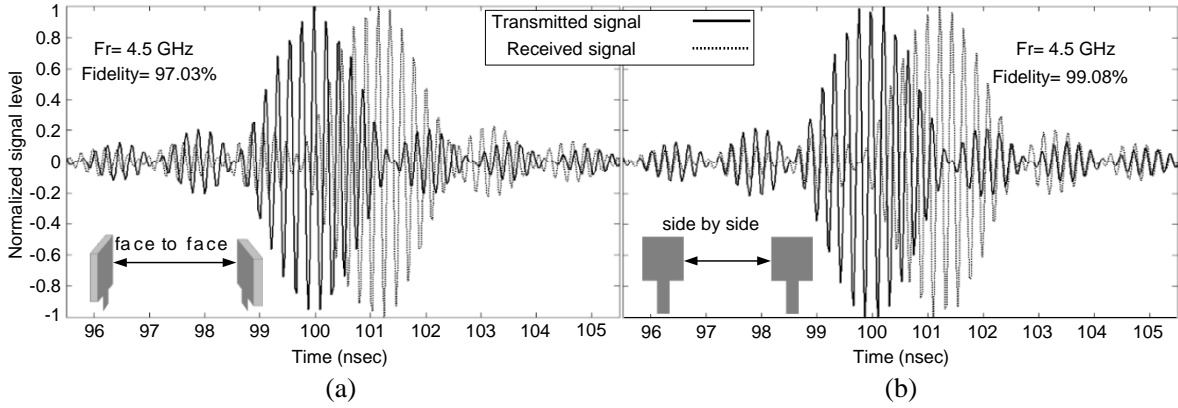


Figure 9. Sync pulses transmitted and received in time domain with two identical (a) face-to-face and (b) side by side the antennas with notches in second frequency band.

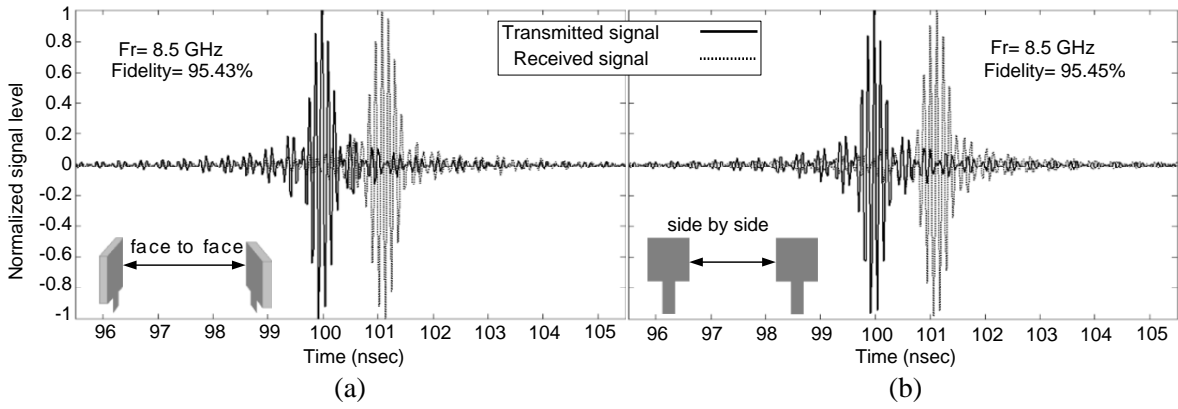


Figure 10. Sync pulses transmitted and received in time domain with two identical (a) face-to-face and (b) side by side the antennas with notches in third frequency band.

signals is evaluated using fidelity factor (7):

$$F = \max_{\tau} \left| \frac{\int_{-\infty}^{+\infty} S(t)r(t - \tau)dt}{\int_{-\infty}^{+\infty} S(t)(2) \cdot \int_{-\infty}^{+\infty} r(t)^2 dt} \right| \quad (7)$$

where $S(t)$ and $r(t)$ are TX and RX signals, respectively. For impulse radio in UWB communications, it is necessary to have a high degree of correlation between TX and RX signals to avoid losing the modulated information. However, for most other telecommunication systems, the fidelity parameter is not that relevant. In order to evaluate the pulse transmission characteristics of the proposed antenna without notch, two configurations (side-by-side and face-to-face orientations) were chosen. The transmitting and receiving antennas were placed in a $d = 25$ cm distance from each other [15]. As shown in Figure 6, although the received pulses in each of the two orientations are broadened, a relatively good similarity exists between the RX and TX pulses. Using (7), the fidelity factor for the face-to-face and side-by-side configurations was obtained equal to 0.98 and 0.96, respectively. These values for the fidelity factor show that the antenna imposes negligible effects on the transmitted pulses. The pulse transmission results are obtained using CST [13]. The fidelities acquired above are for the case that both the antennas were without notch, while for obtaining fidelity of the antenna with two notches, Gaussian pulse cannot be used because it may interfere with notched bands. Unfortunately, there is a wrong procedure in some papers in designing UWB antennas having two notched bands. Fidelities for these antennas with pulses Rayleigh or Gaussian for over frequency band are considered. This subject has been corrected in the paper with introduction of sync pulse (in time domain), and it can be the best solution. According to it, three sync pulses at three various frequencies can be used, and their power spectrum density becomes rectangular. In this case, an interference problem is missed by sync pulse. As exhibited in Figure 7, sync pulses in three different frequencies with their power spectrum density are apparent. It is interesting to note that the frequency band is divided into three bands including 2.3–3.2 GHz, 4.1–4.9 GHz, 7.5–10.3 GHz, respectively. Figures 8, 9, 10 illustrate sync pulses transmitted and received in time domain with two identical notched antennas that have been exposed in a distance of 25 cm in two different positions (face to face, side by side). From the three figures it can be concluded that fidelity factors in all cases are excellent and acceptable (more than 95%). Therefore, the antenna has no any considerable dispersion. With regard to fidelity factor, the antenna in the position side by side seems to be better than the position face to face.

4. FREQUENCY-DOMAIN ANALYSIS

The transmission coefficient S_{21} was simulated in the frequency domain for face-to-face and side-by-side orientations. Figure 11 shows the magnitude and phase S_{21} .

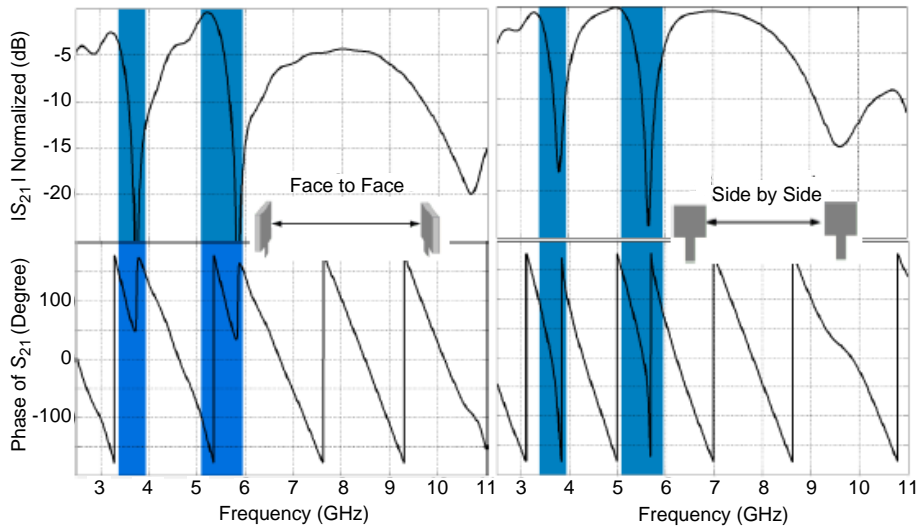


Figure 11. Simulated magnitude and phase of S_{21} with a pair of identical antennas for face to face and side by side orientations.

As it is apparent, magnitude S_{21} is almost flat with variation less than 15 dB in the operating band. The reason of two tangible resonances in magnitude S_{21} is due to two notches WiMAX and

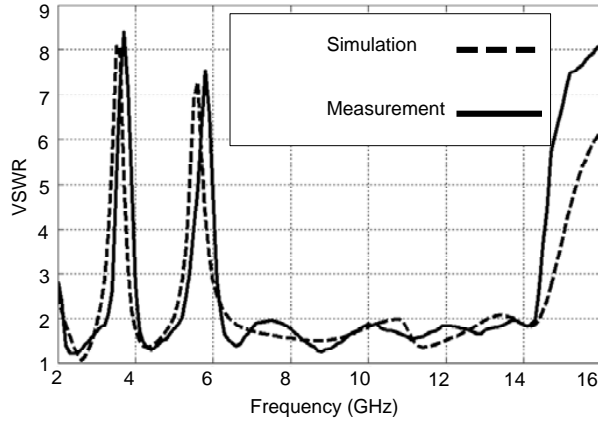


Figure 12. Measured and simulated VSWR versus frequency for the proposed antenna.

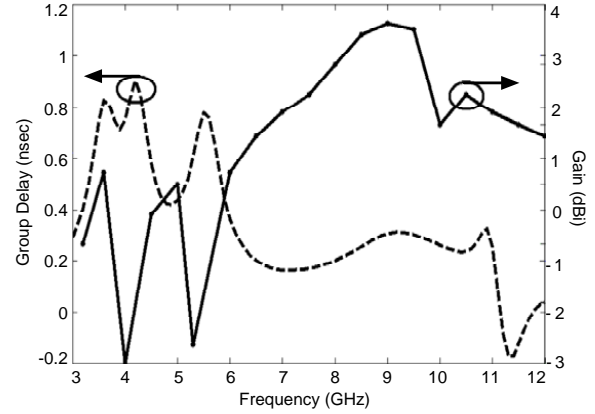


Figure 13. Group delay and measured gain of the antenna.

WLAN bands. Phase of S_{21} for the face-to-face and side-by-side orientations has also been plotted and is shown in Figure 11. As previously expected, the plot shows a linear variation of phase in the total operating band except notched bands. In UWB systems, the information is transmitted using short pulses. Therefore, it is important to study the temporal behavior of the transmitted pulse. The communication system for UWB pulse transmission must limit distortion, spreading and disturbance as much as possible. Group delay is an important parameter in UWB communication, which represents the degree of distortion of pulse signal. The key in UWB antenna design is to obtain a good linearity of phase of the radiated field because the antenna should be able to transmit the electrical pulse with minimal distortion. Usually, the group delay is used to evaluate the phase response of the transfer function because it is defined as the rate of change of the total phase shift with respect to angular frequency. Ideally, when the phase response is strictly linear, the group delay is constant.

$$\text{group delay} = -\frac{d\theta(\omega)}{d\omega} \quad (8)$$

As depicted from Figure 13, the group delay variation is less than 0.7 ns over the frequency band without notched bands which ensure that the pulse transmitted or received by the antenna will not be distorted seriously and will retain its shape. As expected before, there is more the groups delay variation at notches from 3.4–3.69 GHz, and 5.15–5.85 GHz for WiMAX, and WLAN bands compared to other frequencies. Hence, the proposed antenna is useful for modern UWB communication systems.

5. MEASUREMENTS

The VSWR of the antenna has been measured using an Agilent E8362B network analyzer in its full operational span (10 MHz–20 GHz). The antenna is fed through a connector (SMA). The simulated and measured VSWRs of the fabricated antenna are shown in Figure 12. The results show that the antenna impedance bandwidth extends from 2.1 up to 14.3 GHz, as high as 149%. This behavior had before been predicted by HFSS and CST simulations. Good agreement between simulated and measured results is observed, and the little difference between them is attributed to factors such as SMA connector effects, fabrication imperfections and inappropriate quality of the microwave substrate.

The antenna measured gain is obvious in Figure 13 too.

From Figure 13 it is quite clear that the antenna gain decreases down to -3 dBi at two WLAN and WiMAX bands which clearly indicates the effect of the notched bands. The y - z and x - z planes are selected to show the antenna normalized radiation patterns referred to as E -plane and H -plane, respectively. Figure 14 depicts the antenna normalized radiation pattern co-polar at 4 and 9 GHz. It is clear that the proposed antenna has an acceptable quasi omnidirectional pattern required to receive information signals from all directions.

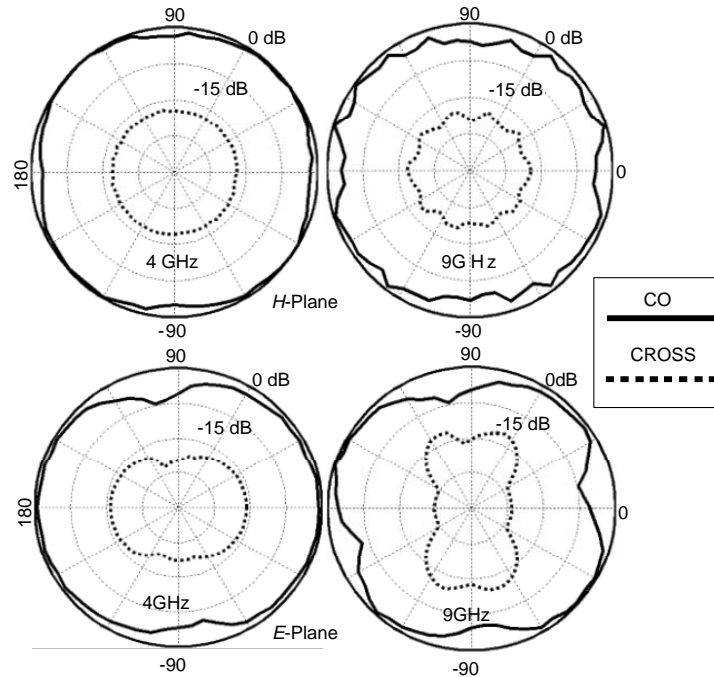


Figure 14. Measured normalized radiation pattern of the antenna.

6. CONCLUSION

A new compact UWB antenna with capability of filtering two interference bands of WiMAX and WLAN was proposed. The results show that VSWR extends from 2.1 up to 14.3 GHz which confirms the antenna UWB characteristic. The antenna was studied in both time and frequency domains. The paper mentions two valuable points. One is the use of the seventh derivative of Gaussian pulse for covering FCC mask, and the other uses sync pulses for obtaining fidelity factor in notched antenna that both achievements increase the value of the paper dramatically.

REFERENCES

1. Huang, C.-Y. and W.-C. Hsia, "Planar elliptical antenna for ultrawideband communications," *Electronics Letters*, Vol. 41, No. 6, 296–297, 2005.
2. Lin, C.-C., Y.-C. Kan, L.-C. Kuo, and H.-R. Chuang, "A planar triangular monopole antenna for UWB communication," *IEEE Microwave and Wireless Components Letters*, Vol. 15, No. 10, 624–626, 2005.
3. Ammann, M. J. and M. John, "Optimum design of the printed strip monopole," *IEEE Antennas and Propagation Magazine*, Vol. 47, No. 6, 59–61, 2005.
4. Liang, J., L. Guo, C. C. Chiau, X. Chen, and C. G. Parini, "Study of CPW-fed circular disc monopole antenna for ultra wide-band applications," *IEE Proceedings: Microwaves, Antennas and Propagation*, Vol. 152, No. 6, 520–526, 2005.
5. Qiao, W., Z. N. Chen, and K. Wu, "UWB monopole antenna with a top-hat sleeve," *International Journal of Microwave and Optical Technology*, Vol. 1, No. 1, 17–27, 2006.
6. Chen, Z. N., T. S. P. See, and X. Qing, "Small printed ultra wideband antenna with reduced ground plane effect," *IEEE Transactions on Antennas and Propagation*, Vol. 55, No. 2, 383–388, 2007.
7. Mighani, M., M. Akbari, and N. Felegari, "A novel SWB small rhombic microstrip antenna with parasitic rectangle into slot of the feed line," *Applied Computational Electromagnetics Society (ACES) Journal*, Vol. 27, No. 1, 74–79, Jan. 2012.

8. Zaker, R., C. Ghobadi, and J. Nourinia, "Bandwidth enhancement of novel compact single and dual band-notched printed monopole antenna with a pair of L-shaped slots," *IEEE Transactions on Antennas and Propagation*, Vol. 57, No. 12, 3978–3983, Dec. 2009.
9. Mighani, M., M. Akbari, and N. Felegari, "A CPW dual band notched UWB antenna," *Applied Computational Electromagnetics Society (ACES) Journal*, Vol. 27, No. 4, 352–359, Apr. 2012.
10. Nezhad, S. A. M. and H. R. Hassani, "A novel triband E-shaped printed monopole antenna for MIMO application," *IEEE Antennas Wirel Propag Lett.*, Vol. 9, 576–579, 2010.
11. Karaboikis, M. P., V. C. Papamichael, G. F. Tsachtsiris, C. F. Soras, and V. T. Makios, "Integrating compact printed antennas onto small diversity/MIMO terminals," *IEEE Transactions on Antennas and Propagation*, Vol. 52, No. 7, 2067–2078, 2008.
12. "Ansoft HFSS user's manual," Ansoft Corporation, Beta Release 11.0, Apr. 2007.
13. CST Microwave Studio, Ver. 2008, Computer Simulation Technology, Framingham, MA, 2008.
14. AWR Design Environment, MWO 2009 Help, 2009.
15. Medeiros, C. R., J. R. Costa, and C. A. Fernandes, "Compact tapered slot UWB antenna with wlan band rejection," *IEEE Antennas And Wireless Propagation Letters*, Vol. 8, 661–664, 2009.